

Sequential Maximum a Posterior (SMAP) Algorithm for Classification of Urban Area using Multi-resolution Spatial Data with Derived Geographical Layers

Uttam Kumar^{1, 2, 3}, Anindita Dasgupta³, Chiranjit Mukhopadhyay¹, and T.V. Ramachandra^{2, 3, 4}

¹Department of Management Studies, ²Centre for Sustainable Technologies, ³Centre for Ecological Sciences, ⁴Centre for *infrastructure*, Sustainable Transport and Urban Planning, Indian Institute of Science, Bangalore – 560012, India.

uttam@ces.iisc.ernet.in, anindita_dasgupta@ces.iisc.ernet.in, cm@mngm.iisc.ernet.in, cestvr@ces.iisc.ernet.in

ABSTRACT

Effective conservation and management of natural resources requires up-to-date information on the land cover (LC) types and their dynamics. Multi-resolution remote sensing (RS) data with appropriate classification strategies have been used to categorise land use and land cover (LULC) of a landscape. RS data coupled with other important environmental layers (both remotely acquired or derived from ground measurements) would be more effective in capturing the LC dynamics and changes associated with the natural resources, as ancillary layers provide additional information that would make the decision boundaries between the LC classes more widely separable, enabling classification with higher accuracy compared to conventional methods of RS data classification. The objective of this paper is to ascertain the possibility of improved classification accuracy of high spatial-low spectral resolution IKONOS data and low spatial-high spectral resolution Landsat ETM+ data of an urban area with the addition of ancillary and derived geographical layers such as vegetation index, temperature, digital elevation model (DEM), aspect, slope and texture.

Results showed that texture played a major role in discriminating individual classes which were rather difficult to distinguish using only original high spatial resolution IKONOS Multispectral (MS) bands. DEM plays a role when the terrain is undulating, however, due to limited vegetation cover, vegetation index was not useful in classification. With ETM+ MS data, inclusion of temperature, NDVI (Normalised Difference Vegetation Index), EVI (Enhanced Vegetation Index), elevation, slope, aspect, Panchromatic band and texture increased the overall accuracy by 7.6% for the same urban area. The study helped in the selection of appropriate ancillary layers for improved classification of RS data depending on the terrain.

Keywords

SMAP, algorithm, IKONOS, Landsat ETM+, urban, classification

1. INTRODUCTION

Classification of remote sensing (RS) data accurately is a prerequisite for many environmental and socio-economic applications [1], such as urban change detection [2-3], urban heat islands [4-6], and estimation of biophysical, demographic, and socio-economic variables [7-8]. Satisfactory classification of RS data depends on many factors including (a) the characteristics of study area, (b) availability of suitable RS data, (c) ancillary and ground reference data, (d) proper use of variables and classification algorithms, (e) user's experience with reference to the application and (f) time constraints [9]. Furthermore, diverse landscapes and terrain types have a mixture of both homogeneous and heterogeneous land cover (LC) classes and require supplemental environmental or geographical layers for improved classification accuracies. Increased spectral variation is common with high degree of spectral heterogeneity in complex landscapes [10]. For example, urban landscapes are composed of features having a complex mix of buildings, roads, flyovers, pavements, trees and lakes which are sometimes smaller than the medium spatial resolution sensors [11]. This creates mixed pixels, a common problem prevalent in residential areas where buildings, trees, lawns, concrete and asphalt all occur within a pixel, often responsible for low classification accuracy, and is a major challenge for selection of suitable image processing approaches over a large area. On the other hand, with the availability of fine spatial resolution data such as IKONOS Multispectral (MS) and Panchromatic (PAN) [12-13], numerous opportunities exist for urban studies. A major advantage is that they reduce the mixed pixel problem, providing the potential to extract much more detailed information of urban structures compared to medium spatial resolution data. However, the most important issue associated with high spatial resolution data is that it is expensive and requires more time for data analysis than medium spatial resolution data [9]. Moreover, high spatial resolution often lead to high spectral variation within the same LC class, and the limited number of spectral bands, including the lack of a shortwave infrared band, leads to a high rate of spectral confusion resulting in poor classification performance [14]. In practice, data acquired from medium spatial resolution sensors

such as Landsat TM/ETM+ or IRS LISS-III, being readily available for multiple dates, are commonly used for urban landscape analysis at a regional scale.

Reducing the spectral variation within the same LC and increasing the separability of different LC types are the keys for improving LC classification [10]. In this regard, different approaches such as sub-pixel classification [15-16], multi-sensor data integration [17], full spectral image classification [18-19], expert classification [20] have been used. Traditional per-pixel spectral-based supervised classification is based only on spectral signatures, but does not make use of rich spatial information inherent in the data [14]. Therefore, making full use of RS information along with ancillary information (acquired or derived environmental layers) would be an efficient way to improve classification accuracy.

The paper is organised as follows: Section 2 highlights the previous work done using additional geographical layers for improving classification accuracy, section 3 states the objectives, and section 4 describes the SMAP classification algorithm. Study area and Data are discussed in section 5, results from IKONOS and Landsat ETM+ are highlighted in section 6, followed by Discussion and Conclusion in section 7 and 8 respectively.

2. LITERATURE REVIEW

There are few earlier studies that show the utility of ancillary and geographically derived data for improving LC classification. Na et al., (2010) [21] used 103 geographical layers to show improvement in LC mapping using Landsat TM bands 1 to 5 and 7, NDVI, EVI, a data fusion transformation combining the six bands information from the Landsat TM image (first principal component – PC1) as additional predictors, image texture measures (variance, homogeneity, contrast, dissimilarity and entropy) with window size of 3 x 3 pixels and 11 x 11 pixels, DEM, slope and soil type with Random Forest (RF), Classification and Regression Tree (CART) and Maximum Likelihood Classifier (MLC) based classification. Among these, RF yielded accurate classification with an overall accuracy of 91% and kappa 0.89. They also quantified the effect of training set size on the performance of classification algorithms. Xiaodong et al., (2009)[22] integrated TM data with NDVI, EVI, first principal component (PC), slope, soil types and five texture measures (variance, homogeneity, contrast, dissimilarity and entropy) for LC classification of Marsh Area using CART and MLC. They concluded that image spectral, textural, terrain data and ancillary Geographical Information System (GIS) improved the land use and land cover(LULC) classification accuracy significantly. Fahsi et al., (2000) [23]evaluated the contribution and quantified the effectiveness of DEM in improving LC classification using Landsat TM data over a rugged area in the Atlas Mountains, Morocco. The study showed that DEM considerably improved the classification accuracy by reducing the effect of relief on

satellite images, increasing the individual accuracies of the different classes by upto 60%.

Recio et al., (2011)[24] used historical land use (LU) and ancillary data as a feature in a geospatial framework for image classification and showed improvement in overall classification accuracy considered case-by-case for each class. Masocha and Skidmore (2011)[25] used DEM along with ASTER imagery and georeferenced point data obtained from field to increase the accuracy of invasive species (*Lantana camera*) mapping. They used Neural Network and SVM classifiers along with GIS expert system to develop hybrid classifiers. The overall accuracy increased from 71% (kappa 0.61) to 83% (kappa 0.77) with Neural Network and from 64% (kappa 0.52) to 76% (kappa 0.67) with SVM hybrid classifiers. Dorren et al., (2003)[26] studied the effect of topographic correction and the role of DEM as additional band using per-pixel and object based classification to classify forest stand type maps using Landsat TM data in a steep mountainous terrain. They concluded that both topographic correction and classification with DEM as additional band increased the overall accuracy.

Xian et al., (2008)[27] quantified multi-temporal urban development characteristics in Las Vegas from Landsat and ASTER Data. Apart from the satellite imageries, NDVI, slope, aspect and temperature were used for classification. Lu and Weng (2005)[9] demonstrated urban classification using full spectral information of Landsat ETM+ imagery in Marion County, Indiana. Role of PC's of ETM+ MS bands, texture, temperature and data fusion of MS and PAN to improve classification accuracy were considered. They concluded that texture and temperature may improve classification accuracy for some classes, but may degrade for other classes. Data fusion of MS and PAN are useful but high spatial resolution also increases spectral variation within the classes, decreasing the classification accuracy. Data fusion combined with texture significantly improved classification accuracy.

3. OBJECTIVE

The objective of this work is to investigate the role of several ancillary and derived layers for high spatial-low spectral resolution IKONOS data and low spatial-high spectral resolution Landsat ETM+ data classification of an urban area with varying characteristics. The following questions are examined in the process of image classification:

- (i.) Does addition of vegetation indices such as NDVI and EVI increase or decrease classification accuracy?
- (ii.) Does elevation and derived layers (slope and aspect) improve classification accuracy?
- (iii.) Does texture has any role in proper identification of classes with better classification accuracy?
- (iv.) How does temperature add to the classification accuracy when included in classification?
- (v.) Does addition of PAN band in addition to MS bands with other ancillary and derived layers prove useful in improving classification accuracy?

4. CONTEXTUAL CLASSIFICATION USING SEQUENTIAL MAXIMUM A POSTERIOR (SMAP) CLASSIFICATION

In SMAP, spectral signatures are extracted from images based on training map by determining the parameters of a spectral class Gaussian mixture distribution model, which are used for subsequent segmentation (i.e. classification) of the MS images. The Gaussian mixture class describes the behavior of an information class which contains pixels with a variety of distinct spectral characteristics. For example, forest, grasslands or urban areas are examples of information classes that need to be separated in an image. However, each of these information classes may contain subclasses each with its own distinctive spectral characteristic; a forest may contain a variety of different tree species each with its own spectral behavior. Mixture classes improve segmentation performance by modelling each information class as a probabilistic mixture with a variety of subclasses. In order to identify the subclasses, clustering is first performed to estimate both the number of distinct subclasses in each class, and the spectral mean and covariance for each subclass. The number of subclasses is estimated using Rissanen's minimum description length (MDL) criteria [28]. This criteria determines the number of subclasses which best describe the data. The approximate maximum likelihood estimates of the mean and covariance of the subclasses are computed using the expectation maximization (EM) algorithm[29-30].

SMAP improves segmentation accuracy by segmenting the image into regions rather than segmenting each pixel separately [31-32]. The algorithm exploits the fact that nearby pixels in an image are likely to have the same class and segments the image at various scales or resolutions using the coarse scale segmentations to guide the finer scale segmentations. In addition to reducing the number of misclassifications, the algorithm generally produces segmentations with larger connected regions of a fixed class. The amount of smoothing that is performed in segmentation is dependent on the behavior of the data. If the data suggest that the nearby pixels often change class, then the algorithm adaptively reduces the amount of smoothing, ensuring that excessively large regions are not formed

(http://wgbis.ces.iisc.ernet.in/grass/grass70/manuals/html70_user/i.smap.html).

5. STUDY AREA AND DATA

The study area selected for urban classification is a part of Greater Bangalore having dense buildup, parks, roads, streets, flyovers, walk ways, open land, etc. Dense and medium urban areas have high surrounding temperature compared to vegetation patches, parks and lakes [6]. The undulating terrain in the city ranges from 735 to 970 m with varying textures due to different urban structures.

IKONOS data (700 x 700 dimension) and Landsat ETM+ MS data pertaining to a part of Greater Bangalore were used for urban classification. Ancillary layers such as elevation and its derived layers such as slope and aspect along with NDVI(Normalised Difference Vegetation Index), EVI (Enhanced Vegetation Index) and textures (ASM - angular second moment, contrast, entropy and variance) were used in separate experiments during classification as summarised in table 1 (for IKONOS data) and table 2 (for Landsat ETM+ data), respectively. Figure 1 shows False Colour Composite (FCC), NDVI, EVI, DEM (Digital Elevation Model), slope and aspect for the study area. EVI values were rescaled from 0 to 1. It is seen from figure 1 that EVI index highlight vegetation better than NDVI (in green colour) compared to FCC. The elevation in this area ranges from 883 to 940 m. Slope and aspect are represented in degrees.

6. RESULTS

6.1 IKONOS data classification

Figure 2 is the output from the eight classifications as explained in table 1 using SMAP. Figure 2 (Classification No. 1) is the classified output of IKONOS 4 bands. Classification No. 2 is the output after adding NDVI as an additional layer to the input in the classifier, where two classes are missing (asbestos roof and open area). Overall, blue plastic roof is over estimated as evident from figure 2 and area statistics in table 3.

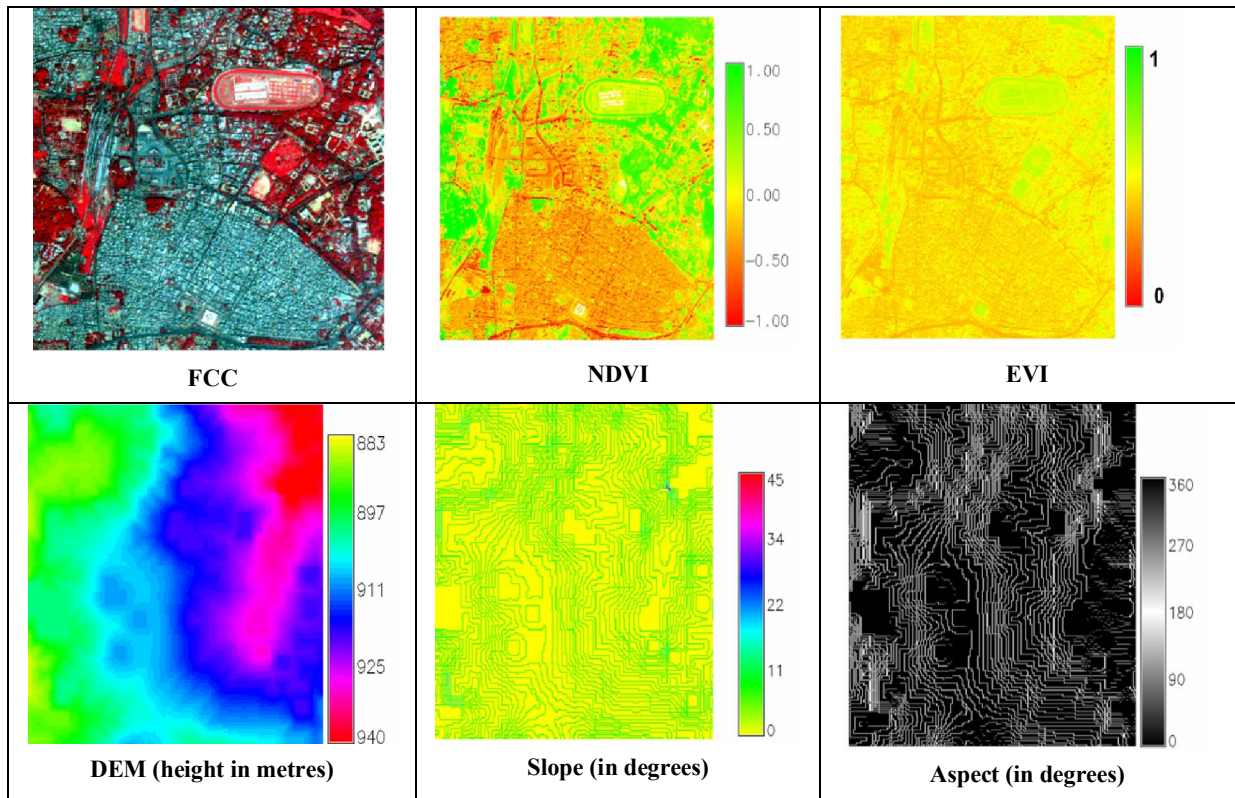


Figure 1. FCC, NDVI, EVI, DEM, slope and aspect added in IKONOS data classification as additional layers.

Table 1. Details of geographical layers used for IKONOS classification

Classification No.	RS data and ancillary geographical layers used	Total number of input layers in the classification
1	IKONOS bands 1, 2, 3, 4	4
2	IKONOS bands 1, 2, 3, 4, and NDVI	5
3	IKONOS bands 1, 2, 3, 4, and EVI	5
4	IKONOS bands 1, 2, 3, 4, and DEM	5
5	IKONOS bands 1, 2, 3, 4, EVI, DEM	6
6	IKONOS bands 1, 2, 3, 4, DEM, slope and aspect	7
7	IKONOS bands 1, 2, 3, 4, DEM, slope, aspect and EVI	8

8	IKONOS bands 1, 2, 3, 4, DEM and Texture (ASM, contrast, entropy, variance) at 0, 45, 90 and 135 degrees for IKONOS bands 1, 2, 3, 4	$5+(4 \times 4 \times 4) = 69$
---	--	--------------------------------

The role of NDVI in discriminating non-vegetation area is negligible and therefore asbestos and open areas have merged with concrete roof and blue plastic with a drastic decrease in overall accuracy (47%) as shown in table 4. When EVI was added as an additional derived layer, classification is better compared to the inclusion of NDVI. However, the class composition is either under estimated (concrete roof, vegetation and open area) or over estimated (blue plastic roof) lowering the overall accuracy to 55%. Blue plastic roof was also over estimated when both EVI and DEM were added as input layers along with the original bands. As evident from figure 2, concrete roof and open area have been misclassified and merged to blue plastic roof, which is dominant in the scene. Asbestos roof and vegetation are the two classes which showed higher producer's and user's accuracies. However, the overall accuracy still remained low (49.28%).

Similar situation prevails when DEM, slope and aspect were included with the input IKONOS MS bands to the

classifier. Concrete roof, open area and vegetation are under estimated and blue plastic roof is over estimated, bringing the overall accuracy to as low as 55%. The output worsens when DEM, slope, aspect with EVI were considered additionally to the input. All the classes are either over estimated or under estimated with overall accuracy of 51% (table 4). In classification No. 8, when only DEM and texture measures were added (table 1) as input to the classifier apart from IKONOS 4 MS bands, the overall accuracy went high to 88.72% with high producer's and user's accuracies for individual classes which were classified properly (table 3).

The above experiments conclude that in a highly urbanised area with less vegetation cover and highly contrasting features, texture plays a major role in discriminating individual classes which are rather difficult to distinguish using only original high

Table 2. Details of data and ancillary layers used for Landsat ETM+ MS classification

Classification No.	RS data and ancillary geographical layers used	Total number of input layers in the classification
1	ETM+ bands 1, 2, 3, 4, 5 and 7 at 30 m	6
2	ETM+ bands 1, 2, 3, 4, 5, 7 and Temperature	7
3	ETM+ bands 1, 2, 3, 4, 5, 7, NDVI, EVI, elevation, slope and aspect	11
4	ETM+ bands 1, 2, 3, 4, 5, 7, Temperature, NDVI, EVI, elevation, slope and aspect	12
5	ETM+ bands 1, 2, 3, 4, 5, 7, Temperature, NDVI, EVI, elevation, slope and aspect, texture (ASM, contrast, entropy, variance) at 0, 45, 90 and 135 degrees for ETM+ bands 1, 2, 3, 4, 5, 7	108
6	ETM+ bands 1, 2, 3, 4, 5, 7, Temperature, NDVI, EVI, elevation, slope and aspect, texture (ASM, contrast, entropy, variance) at 0, 45, 90 and 135 degrees for ETM+ bands 1, 2, 3, 4, 5, 7	109
7	ETM+ bands 1, 2, 3, 4, 5, 7, Temperature, NDVI, EVI, ETM+ PAN, texture (ASM, contrast, entropy, variance) at 0, 45, 90 and 135 degrees for ETM+ bands 1, 2, 3, 4, 5, 7, and ETM+ PAN elevation, slope and aspect	125

spatial resolution IKONOS MS bands as evident from high classification accuracies in table 4 (Classification No. 4 and 8 highlighted in bold), compared to the classification of only IKONOS 4 MS bands (Classification No. 1 highlighted in bold). DEM plays a role when the terrain is undulating but derived layers such as slope and aspect did not aid in discriminating classes when the elevation had low variance. Due to limited vegetation presence (a few parks) in the study area, EVI was not useful in classification. Overall 3.5% improvement in accuracy was observed after including elevation and texture along with the original bands as input to the classifier.

6.2 Landsat ETM+ data classification

Seven separate classifications were carried out with the different combinations of Landsat ETM+ bands and geographical layers as summarised in table 2. Landsat ETM+ PAN band was also added in the classification data set and the other 6 MS bands were resampled to 15 m. Finally, the texture measures from PAN band were included as input to classification, making the total number of geographical layers to 125. Figure 3 shows output from the seven classified images and LU statistics are listed in table 5. The producer's, user's, overall accuracies and kappa are given in table 6.

Figure 3 indicates that outputs obtained from the original spectral bands along with temperature, NDVI, EVI, elevation, slope and aspect (Classification No. 1, 2, 3 and 4) have misclassified many pixels belonging to builtup, water and open area. Many of the tarred or concrete road pixels that actually belong to builtup have been classified as water. Thus water class has been over estimated.

Addition of texture, PAN band and texture of PAN significantly improved the classification accuracy of all the classes including urban and water bodies as evident from table 5 (highlighted in bold). From accuracy assessment in table 6, we see that Classification No. 5, 6 and 7 have higher accuracies compared to other classifications. Inclusion of temperature increased accuracy whereas addition of vegetation index layers along with elevation, slope and aspect decreased the overall accuracy. When both temperature and vegetation index with elevation, slope and aspect were used, the accuracy still decreased. However, inclusion of texture and PAN significantly increased the overall accuracy. There was a 7.6% increase in accuracy by adding temperature, NDVI, EVI, elevation, slope, aspect, PAN along with texture measures, which proved to be useful for mediumspatial resolution data such as ETM+ while discriminating different classes in an urban environment.

7. DISCUSSION

Analysis of the role of ancillary and derived geographical layers in improving classification accuracy is required along with the new methods of expert classification being developed [25]. In this work, derived and ancillary layers were assessed for their

performance in improving classification accuracy in an urbanised landscape.

The results provided new insights to the likelihood of improved performance of LC classification by use of supplemental layers related to the region along with the RS data. IKONOS data were used for urban area classification along with many other layers of elevation and texture. The enhanced characteristics of IKONOS MS and PAN compared to Landsat ETM+ highlighted some typical urban features such as buildings and narrow roads in residential areas compared to the latter (figure

3). IKONOS image not only reduced the mixed pixel problem, but also provided a rich texture and contextual information than Landsat ETM+ MS bands with 15 or 30 m spatial resolution. Earlier works [33-34] have used SPOT HRV data for urban classification due to its high spatial resolution comparing with Landsat ETM data. Knowledge based expert system have also been used with MS imagery and LiDAR data to delineate impervious surface in urban areas [35]. The study showed that high spatial resolution is considered to be more important than high spectral resolution in urban classification [1].

Table 3. Area statistics from the IKONOS classified images

Class → Area ↓		Concrete roof	Asbestos roof	Blue plastic roof	Vegetation	Open area	Total
Classification No. 1	ha	351.74	9.53	1.88	260	158.80	781.76 ha (100%)
	%	44.99	1.22	0.24	33.26	20.66	
Classification No. 2	ha	324.51	-	285.02	172.23	-	
	%	41.51	-	36.46	22.03	-	
Classification No. 3	ha	299.89	7.26	259.32	188.17	27.11	
	%	38.36	0.93	33.17	24.07	3.47	
Classification No. 4	ha	352.74	8.82	1.42	259.98	161.49	
	%	44.96	1.12	0.18	33.14	20.59	
Classification No. 5	ha	84.53	11.20	385.11	244.86	56.06	
	%	10.81	1.43	49.26	31.32	7.17	
Classification No. 6	ha	142.56	17.44	331.30	218.02	72.44	
	%	18.24	2.23	42.38	27.89	9.27	
Classification No. 7	ha	126.17	16.13	433.22	146.88	59.36	
	%	16.14	2.06	55.42	18.79	7.59	
Classification No. 8	ha	354.88	7.93	0.95	259.33	158.66	
	%	45.40	1.22	0.12	33.17	20.30	

Table 4. Accuracy assessment of the IKONOS classified images

lass → Accuracy ↓	Concrete roof	Asbestos roof	Blue plastic roof	Vegetation	Open area	Overall Accuracy	Kappa
Classification No. 1							
Producer's accuracy (%)	92.50	89.15	85.00	85.00	76.92	85.25	0.8250
User's accuracy (%)	89.99	81.00	87.00	83.00	83.00		
Classification No. 2							
Producer's accuracy (%)	76.22	-	17.01	48.55	-	47.63	0.4136
User's accuracy (%)	69.45	-	21.97	51.33	-		
Classification No. 3							
Producer's accuracy (%)	83.77	91.34	10.55	48.00	18.00	55.05	0.5117
User's accuracy (%)	70.53	97.63	42.31	41.38	17.09		
Classification No. 4							
Producer's accuracy (%)	90.15	87.48	84.53	82.07	86.18	86.21	0.8437
User's accuracy (%)	87.57	84.39	85.11	85.95	88.79		
Classification No. 5							
Producer's accuracy (%)	42.89	73.94	10.05	78.53	55.91	49.28	0.4577
User's accuracy (%)	22.05	75.9	19.23	83.91	30.37		
Classification No. 6							
Producer's accuracy (%)	57.55	67.58	18.06	78.66	57.81	55.37	0.5322
User's accuracy (%)	55.04	72.55	21.23	73.84	51.41		
Classification No. 7							
Producer's accuracy (%)	58.38	51.43	12.05	76.25	65.99	51.06	0.4719
User's accuracy (%)	51.31	58.45	17.69	64.37	54.70		
Classification No. 8							
Producer's	92.57	89.25	89.00	86.13	88.37	88.72	0.8615

accuracy (%)						
User's accuracy (%)	90.00	82.00	88.00	90.15	91.75	

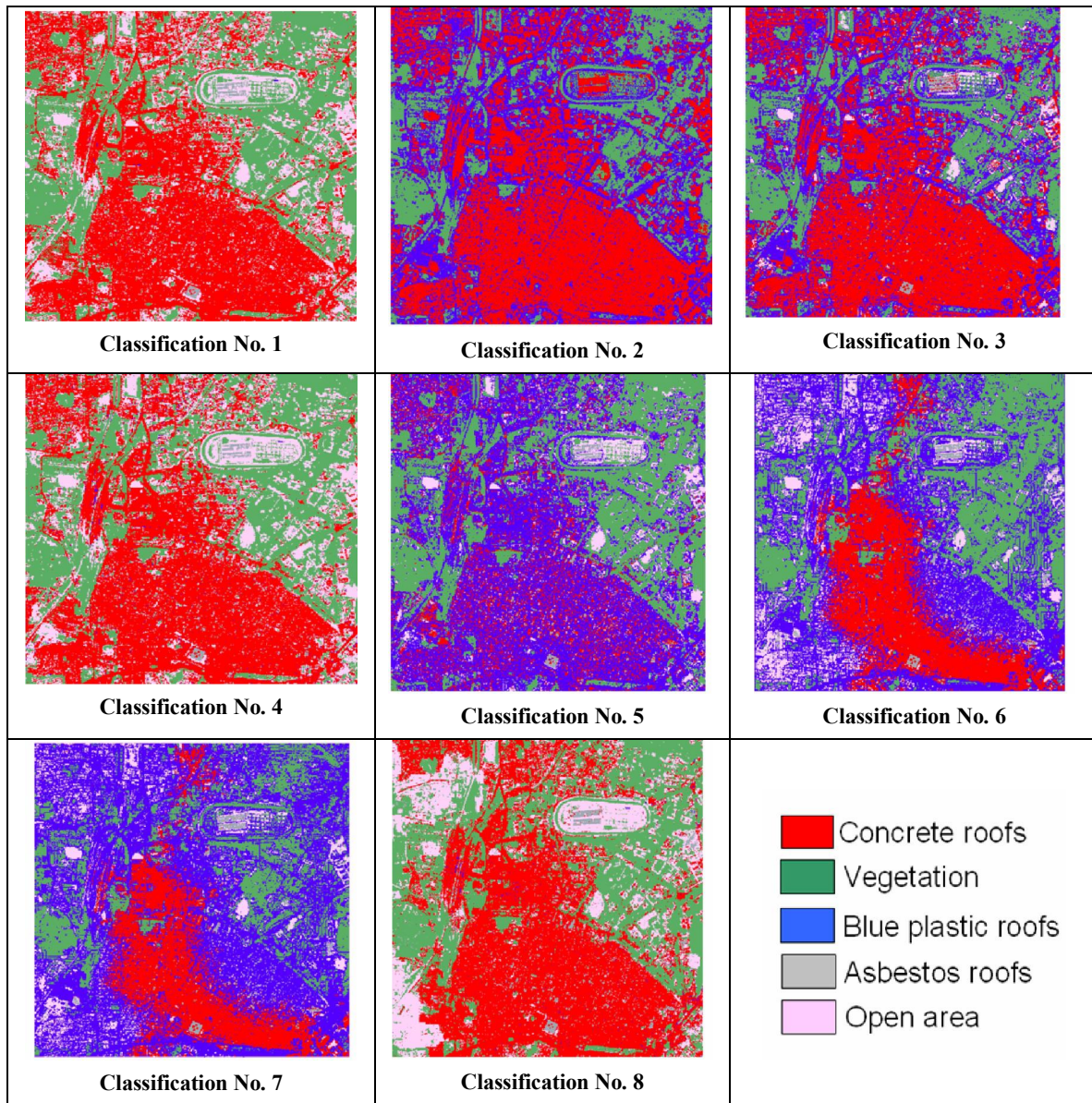


Figure 2. Classified outputs from IKONOS by adding additional geographical layers.

In IKONOS data classification, when only DEM and texture measures were added as input to the classifier apart from IKONOS 4 spectral bands, the overall accuracy went high to 88.72% (3.5% improvement) with high producer's and user's

accuracies for individual classes, which is comparable to the overall accuracy obtained by classifying QuickBird imagery for LC classification in a complex urban environment based on texture (overall accuracy – 87.33%) and segmentation (overall

accuracy – 88.33%) by Lu et al., (2010) [14]. Although it is difficult to identify suitable texture which is dependent on image band and window size for the specific study[36], appropriate texture measures reduce spectral variation within same LC and also improves spectral separability among different LC classes [37-40]. It is to be noted that derived layers from elevation such as slope and aspect did not aid in discriminating classes and EVI did not prove useful in classification due to poor vegetation cover. Addition of temperature, NDVI, EVI, elevation, slope,

aspect, PAN and texture with Landsat ETM+ spectral bands 1, 2, 3, 4, 5 and 7, significantly improved the classification accuracy by 7.6%, which proved to be useful with medium spatial resolution data in an urban area.

However, in addition to the use of ancillary layers such as textural images, selection of different seasonal images along with suitable classification algorithms are also needed to improve classification performance[14].

Table 5. Area statistics from the Landsat ETM+ classified images

Class → Area ↓		Urban	Vegetation	Water	Open area	Total
Classification 1	ha	4543.14	1911.89	600.32	1999.25	9054.62 ha (100%)
	%	50.17	21.12	6.63	22.08	
Classification 2	ha	4014.78	1825.96	560.71	2653.15	
	%	44.34	20.17	6.19	29.30	
Classification 3	ha	4245.71	1884.53	471.43	2446.04	
	%	46.93	20.83	5.21	27.03	
Classification 4	ha	3450.37	1854.25	554.54	3188.55	
	%	38.14	20.49	6.13	35.24	
Classification 5	ha	5262.71	1905.61	93.96	1754.99	
	%	58.36	21.13	1.04	19.46	
Classification 6	ha	5226.04	1887.87	86.47	1816.89	
	%	57.96	20.94	0.96	20.15	
Classification 7	ha	5164.41	1974.06	65.70	1813.11	
	%	57.27	21.89	0.73	20.11	

8. CONCLUSION

RS based LC mapping and monitoring of large areas has created new challenge with the varied spatial scale and data volume, requiring automated classification algorithms that minimise human interventions. This work has shown that use of spatial information along with ancillary and derived geographical layers is an effective way to improve LC classification performance which was demonstrated in an urban terrain.

In a highly urbanised area with less vegetation cover and highly contrasting features, texture played a major role in discriminating individual classes which were rather difficult to distinguish using only original high spatial resolution IKONOS MS bands. DEM plays a role when the terrain is undulating, however, due to limited vegetation cover, vegetation index was not useful in classification. For the same urban area, inclusion of temperature, NDVI, EVI, elevation, slope, aspect, PAN and texture significantly increased the overall accuracy by 7.6% while discriminating different classes properly with Landsat ETM+ data.

9. ACKNOWLEDGMENTS

We thank GeoEye Foundation, USA for providing IKONOS imagery for Greater Bangalore city. We are grateful to NRDMS Division, DST, The Ministry of Science and Technology, Government of India and Indian Institute of Science for the financial assistance and infrastructure support.

10. REFERENCES

- [1] Jensen, J. R., and Cowen, D. C., 1999. Remote sensing of urban/suburban infrastructure and socioeconomic attributes. *Photogrammetric Engineering and Remote Sensing*. vol. 65, 611-622.
- [2] Ward, D., Phinn, S. R., and Murray, A. L., 2000. Monitoring growth in rapidly urbanizing areas using remotely sensed data. *Professional Geographer*. vol. 53, 371-386.
- [3] Ramachandra T. V. and Kumar, U., 2008. Wetlands of Greater Bangalore, India: Automatic Delineation through Pattern Classifiers. *The Greendisk Environmental Journal, (International Electronic Journal)*. vol. 1(26), 1-22.

- [4] Lo, C. P., Quattrochi, D., and Luvall, J., 1997. Application of high resolution thermal infrared remote sensing and GIS to assess the urban heat island effect. *International Journal of Remote Sensing*. vol. 18, 287-304.
- [5] Weng, Q., 2001. A remote sensing-GIS evaluation of urban expansion and its impact on surface temperature in the ZhujiangDelta, China. *International Journal of Remote Sensing*. vol. 22, 1999-2014.
- [6] Ramachandra T. V., and Kumar, U., 2009. Land Surface Temperature with Land Cover Dynamics: Multi-Resolution, Spatio-Temporal Data Analysis of Greater Bangalore. *International Journal of Geoinformatics*, vol. 5(3), 43-53.
- [7] Lo, C. P., 1995. Automated population and dwelling unit estimation from high-resolution satellite images: a GIS approach. *International Journal of Remote Sensing*, vol. 16, 17-34.
- [8] Thomson, C. N., and P. Hardin, 2000. Remote sensing/GIS integration to identify potential low-income housing sites. *Cities*, vol. 17, 97-109.
- [9] Lu, D., and Weng, Q., 2005. Urban Classification Using Full Spectral Information of Landsat ETM+ Imagery in MarionCounty, Indiana. *Photogrammetric Engineering and Remote Sensing*. vol. 71(11), 1275-1284.
- [10] Lu, D., and Weng, Q., 2007. A survey of image classification methods and techniques for improving classification performances. *International Journal of Remote Sensing*, vol. 28(5), 823-870.
- [11] Jensen, J. R., 2000. An Earth Resource Perspective, Prentice Hall, Upper Saddle River, New Jersey. *Remote Sensing of the Environment*. 544.
- [12] Sugumaran, R., Zerr, D., and Prato, T., 2002. Improved urban land cover mapping using multitemporal Ikonos images for local government planning, *Canadian Journal of Remote Sensing*. vol. 28, 90-95.
- [13] Van der Sande, C. J., de Jong, S. M., and de Roo, A. P. J., 2003. A segmentation and classification approach of IKONOS-2 imagery for land cover mapping to assist flood risk and flood damage assessment. *International Journal of Applied Earth Observation and Geoinformation*. vol. 4, 217-229.
- [14] Lu, D., Hetrick, S., and Moran, E., 2010. Land Cover Classification in a Complex Urban-Rural landscape with Quickbird Imagery. *Photogrammetric Engineering and Remote Sensing*. vol. 76(10), 1159-1168.
- [15] Rashed, T., Weeks, J. R., Gadalla, M. S., and Hill, A. G., 2001. Revealing the anatomy of cities through spectral mixture analysis of multispectral satellite imagery: a case study of the Greater Cairo region, Egypt. *Geocarto International*. vol. 16, 5-15.
- [16] Lu, D., Mausel, P., Batistella, M., and Moran, E., 2004a. Comparison of land-cover classification methods of the Brazilian Amazon Basin. *Photogrammetric Engineering and Remote Sensing*. vol. 70, 732-731.
- [17] Haack, B. N., Solomon, E. K., Bechdol, M. A., and Herold, N. D., 2002. Radar and optical data comparison/integration for urban delineation: a case study. *Photogrammetric Engineering and Remote Sensing*. vol. 68, 1289-1296.
- [18] Stuckens, J., Coppin, P. R., and Bauer, M. E. 2000. Integrating contextual information with per-pixel classification for improved land cover classification. *Remote Sensing of Environment*. vol. 71, 282-296.
- [19] Shaban, M. A., and Dikshit, O., 2001. Improvement of classification in urban areas by the use of textural features: the case study of Lucknow city, Uttar Pradesh. *International Journal of Remote Sensing*. vol. 22, 565-593.
- [20] Hung, M., and Ridd, M. K., 2002. A subpixel classifier for urban land-cover mapping based on a maximum-likelihood approach and expert system rules. *Photogrammetric Engineering and Remote Sensing*. vol. 68, 1173-1180.
- [21] Na, X., Zhang, S., Li, Xiaofeng, Yu, H., and Liu, C., 2010. Improved Land Cover Mapping using Random Forests Combined with Landsat Thematic Mapper Imagery and Ancillary Geographic Data. *Photogrammetric Engineering and Remote Sensing*. vol. 76(7), 833-840.
- [22] Xiaodong, Na, Shuqing, Z., Huaiqing, Z., Xiaofeng, L., Chunyue, L., 2009. Integrating TM and Ancillary Geographical Data with Classification Trees for Land Cover Classification of Marsh Area. *Chinese Geographical Science*. vol. 19(2), 177-185.
- [23] Fahsi, A., Tsegaye, T., Tadesse, W., and Coleman, T., 2000. Incorporation of digital elevation models with Landsat-TM data to improve land cover classification accuracy. *Forest Ecology and Management*. vol. 128(2000), 57-64.
- [24] Recio, J. A., Hermosilla, L. A., and Fernandez-Sarria, A., 2011. Historical Land Use as a Feature for Image Classification. *Photogrammetric Engineering and Remote Sensing*. vol. 77(4), 377-387.
- [25] Masocha, M., and Skidmore, A. K., 2011. Integrating conventional classifiers with a GIS expert system to increase the accuracy of invasive species mapping. *International Journal of Applied Earth Observation and Geoinformation*. vol. 13, 487-494.
- [26] Dorren, L. K. A., Maier, B., Seijmonsbergen, A. C., 2003. Improved Landsat-based forest mapping in steep mountainous terrain using object-based classification. *Forest Ecology and Management*. vol. 183(2003), 31-46.
- [27] Xian, G., Crane, M., and McMahon, C., 2008. Quantifying Multi-temporal Urban development Characteristics in Las Vegas from Landsat and ASTER Data. *Photogrammetric Engineering and Remote Sensing*. vol. 74(4), 473-481.
- [28] Rissanen, J., 1983. A Universal Prior for Integers and Estimation by Minimum Description Length. *Annals of Statistics*. vol. 11(2), 417-431.

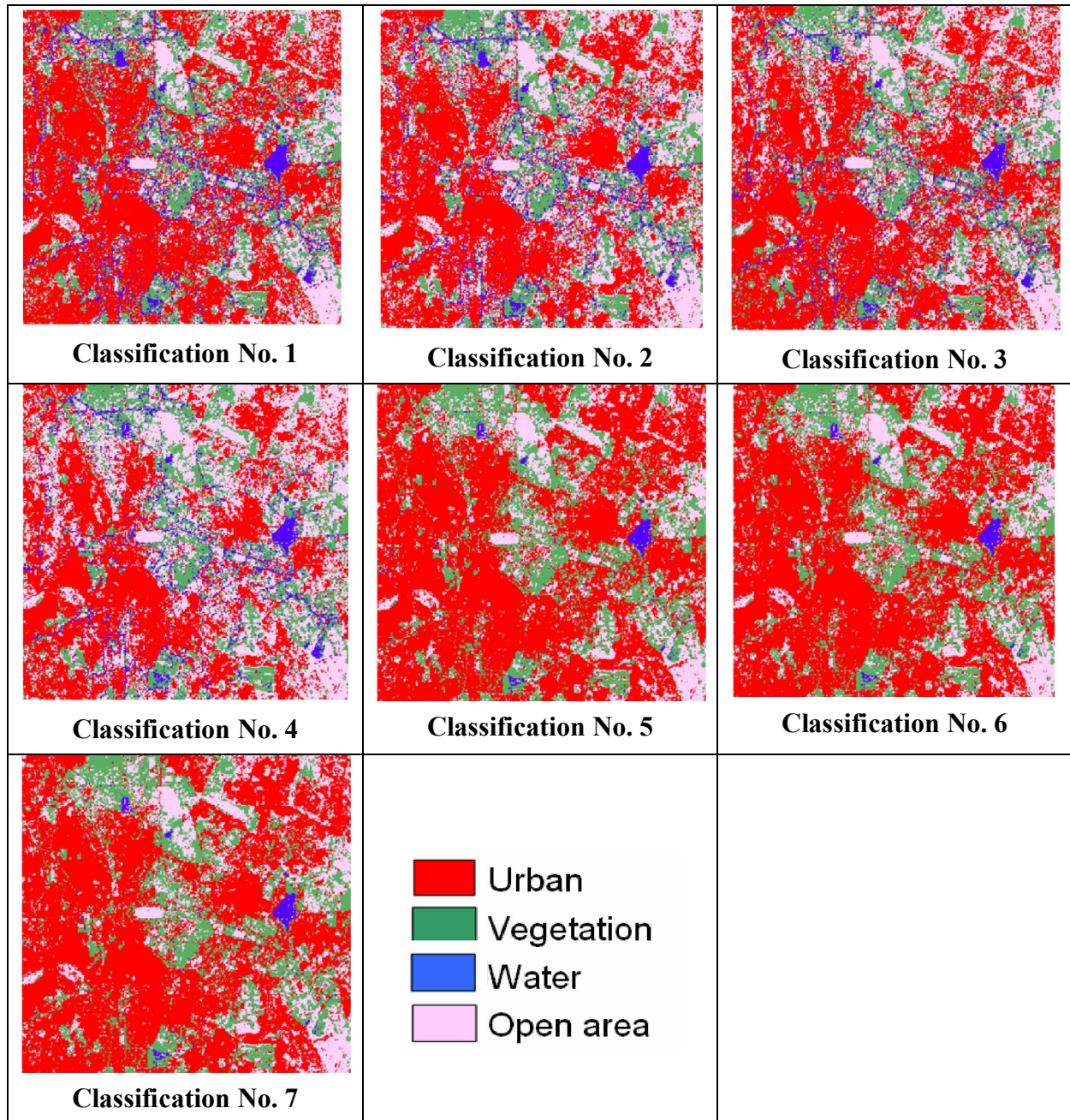


Figure 3. Classified outputs from Landsat ETM+ bands by adding additional geographical layers.

Table 6. Accuracy assessment of the Landsat ETM+ classified images

Class → Accuracy ↓	Urban	Vegetation	Water	Open area	Overall Accuracy	Kappa
Classification No. 1						
Producer's accuracy (%)	73.94	87.45	66.91	74.62	75.50	0.7309
User's accuracy (%)	76.92	84.36	61.00	78.82		
Classification No. 2						
Producer's accuracy (%)	76.22	87.99	68.62	79.52	77.94	0.7548
User's accuracy (%)	78.73	83.05	65.28	81.03		
Classification No. 3						
Producer's accuracy (%)	71.88	78.87	69.96	71.09	73.12	0.7101
User's accuracy (%)	74.70	77.95	65.23	75.29		
Classification No. 4						
Producer's accuracy (%)	68.33	81.87	57.34	77.11	71.43	0.6811
User's accuracy (%)	75.19	78.33	59.61	72.55		
Classification No. 5						
Producer's accuracy (%)	83.57	82.41	78.91	81.88	81.84	0.7978
User's accuracy (%)	83.64	83.37	80.85	81.76		
Classification No. 6						
Producer's accuracy (%)	83.99	82.59	79.15	82.13	82.29	0.8077
User's accuracy (%)	83.94	83.77	81.17	82.44		
Classification No. 7						
Producer's accuracy (%)	84.91	88.21	81.11	83.62	83.15	0.8125
User's accuracy (%)	81.17	81.57	84.23	80.51		

- [29] Dempster, A., Laird, N., and Rubin, D., 1977. Maximum Likelihood from Incomplete Data via the EM Algorithm. *Journal of the Royal Society Series B of Statistics*.vol. 39(1), 1-38.
- [30] Redner, E., and Walker, H., 1984. Mixture Densities, Maximum Likelihood and the EM Algorithm. *SIAM Review*.vol. 26(2), 195-239.
- [31] Bouman, C., and Shapiro, M., 1992. Multispectral Image Segmentation using a Multiscale Image Model. In *Proceedings of IEEE International Conference on Acoust., Speech and Signal Processing* (San Francisco, California, March 23-26, 1992). pp. III-565-III-568.
- [32] Bouman, C. and Shapiro, M., 1994. A Multiscale Random Field Model for Bayesian Image Segmentation. *IEEE Transaction on Image Processing*. vol. 3(2), 162-177.URL: http://wgbis.ces.iisc.ernet.in/grass/grass70/manuals/html70_user/i_smap.html
- [33] Gong, P., Marceau, D. J., and Howarth, P. J., 1992. A comparison of spatial feature extraction algorithms for land-use classification with SPOT HRV data. *Remote Sensing of Environment*. vol. 40, 137-151.
- [34] Shaban, M. A., and Dikshit, O., 2002. Evaluation of the merging of SPOT multispectral and panchromatic data for classification of an urban environment. *International Journal of Remote Sensing*. vol. 23, 249-262.
- [35] Germaine, K. A., and Hung, M-C., 2011. Delineation of Impervious Surface from Multispectral Imagery and Lidar Incorporating Knowledge Based Expert System Rules. *Photogrammetric Engineering and Remote Sensing*. vol. 77(1), 75-85.
- [36] Chen, D., Stow, D.A., and Gong, P., 2004. Examining the effect of spatial resolution and texture window size on classification accuracy: an urban environment case. *International Journal of Remote Sensing*. vol. 25, 2177-2192.
- [37] Haralick, R. M., K. Shanmugam, and I.Dinstein, 1973. Textural features for image classification. *IEEE Transactions on Systems, Man, and Cybernetics, SMC*. vol. 3(6), 610-621.
- [38] Augera, F., Aguilar, F. J., and Aguilar, M. A., 2008. Using texture analysis to improve per-pixel classification of very high resolution images for mapping plastic greenhouses. *ISPRS Journal of Photogrammetry and Remote Sensing*. vol. 63, pp. 635-646.
- [39] Lu, D., Batistella, M., and Moran, E., 2008a. Integration of Landsat TM and SPOT HRG Images for Vegetation Change Detection in the Brazilian Amazon. *Photogrammetric Engineering and Remote Sensing*, vol. 74(4), 421-430.
- [40] Lu, D., Batistella, M., Moran, E., and de Miranda, E. E., 2008b. A comparative study of Landsat TM and SPOT HRG images for vegetation classification in the Brazilian Amazon. *Photogrammetric Engineering and Remote Sensing*. vol. 70(3), 311-321.